International Journal of Innovative Computing, Information and Control
Volume **8**, Number **9**, September **2012**

ICIC International ©2012 ISSN 1349-4198
pp. 6357–6370

DISCRETE-TIME ADAPTIVE CONTROL OF NONLINEAR BASE ISOLATED STRUCTURES

Francesc Pozo[1], José Rodellar[2] and Mohammed Ismail[3]

[1]CoDAlab, Departament de Matemàtica Aplicada III
Escola Universitària d'Enginyeria Tècnica Industrial de Barcelona
Universitat Politècnica de Catalunya
Comte d'Urgell, 187, 08036 Barcelona, Spain
francesc.pozo@upc.edu

[2]CoDAlab, Departament de Matemàtica Aplicada III
Escola Tècnica Superior d'Enginyers de Camins, Canals i Ports de Barcelona
Universitat Politècnica de Catalunya
Jordi Girona, 1-3, 08034 Barcelona, Spain
jose.rodellar@upc.edu

[3]Structural Engineering Department
Zagazig University
44519 Zagazig, Egypt
mohammed.ismail@upc.edu

Received March 2011; revised July 2011

Abstract. *This paper deals with an active control system for base isolated structures. The isolator device has a hysteretic nonlinear behavior. An adaptive backstepping approach is used for the control design in order to handle the nonlinearity and the presence of uncertainties. The control is formulated in continuous time and further discretized into a discrete time control algorithm to go closer to a digital implementation. The paper shows that the implementation of this algorithm with a zero-order hold is able to keep uniformly all the signals of the closed loop within certain bounds and to give an upper bound of the asymptotic tracking error.*
Keywords: Backstepping, Discrete-time control, Base-isolated structures, Hysteresis

1. **Introduction.** Combinations of passive devices with active or semi-active feedback controllers have been proposed in recent years in the framework of smart base isolated structures [1-5]. The feasibility of adding a feedback control system to a passive design is based on the premise that only a control action is to be applied at the base with force magnitudes which are not excessive due to the high flexibility of the isolators. The benefits of the inclusion of the control lie mainly in that the application of this force can avoid large displacements of the base isolator, which could endanger the scheme integrity; and it may also introduce an additional resistant scheme not dependable of the inter-story drifts, which are already small due to the effect of the isolator. This may be useful, particularly for structures having sensitive installations, like hospitals, public services and computer facilities.

One of the conceptual challenges for the development of a control law is associated with the nonlinear behavior of the base isolators and with the uncertainties in the model describing the structure-base-isolator system and in the seismic excitation. Robust nonlinear control laws have been proposed by [1,6-10]. Recently a new tool has been proposed in the control theory to design nonlinear schemes for uncertain systems [11]. Backstepping is an appealing alternative since it gives computable explicit bounds for the closed loop

tracking error as a function of the size of the uncertainties [12]. A backstepping controller for a base isolation scheme has been recently proposed by [13].

Usually the control law design is performed based on a continuous time model of the system to be controlled and the resulting controller has a continuous time mathematical structure. Since the control law is to be finally implemented through a digital control system, a discrete time control algorithm has to be obtained. The pure discretization of the continuous control law is a common practice and intuition says that, if the sampling period is small enough, the performance of the discrete version of the controller will meet the theoretical continuous performance with a reasonable error. However, this intuition has been only proved in a few cases. The reference by [14] gave a prove that a discretization of a backstepping controller is able to stabilize a continuous time system under some conditions. In this paper, this approach is used to formulate a discretized version of the hybrid controller of [13]. In this work we consider two different systems: a base isolated single degree of freedom model and an eight-storied building structure. The first one is used as a model for the design of the control algorithm and as a first test of its effectiveness. The second one is used to perform a more extensive assessment on a more realistic case. In the implementation of the control algorithm, special attention is given to some issues related to the joint selection of the sampling period and controller parameters.

2. **Design Models.** Consider a base isolated structure with an active controller as illustrated in Figure 1. The passive component consists of a hysteretic base isolator.

The whole system can be described by a model composed of two coupled systems: Σ_s (the structure) and Σ_b (the base).

The absolute equations of motion are the following:

$$\Sigma_b^a: \quad m_1\ddot{x}_1 + (c_1+c_2)\dot{x}_1 + (k_1+k_2)x_1 = k_2x_2 + c_2\dot{x}_2 - \Phi(x_1-d,t) + c_1\dot{d} + k_1d + u \tag{1}$$

$$\Sigma_s^a: \quad m_2\ddot{x}_2 + c_2\dot{x}_2 + k_2x_2 - c_2\dot{x}_1 - k_2x_1 = 0 \tag{2}$$

where m_1 and m_2 are the mass of the base and the structure, respectively; c_1 and c_2 are the damping coefficients; k_1 and k_2 are the stiffness coefficients; x_1 and x_2 are the absolute displacement of the base and the structure, respectively; the excitation is produced by a horizontal seismic ground motion characterized by an inertial displacement $d(t)$, velocity $\dot{d}(t)$ and acceleration $\ddot{d}(t)$; the base displacement relative to the ground is $y_1 = x_1 - d$, while $y_2 = x_2 - d$ is the relative structure displacement; Φ is the restoring force characterizing the hysteretic behavior of the isolator material, which is usually made with inelastic rubber bearings; and u is the control force supplied by an appropriate actuator.

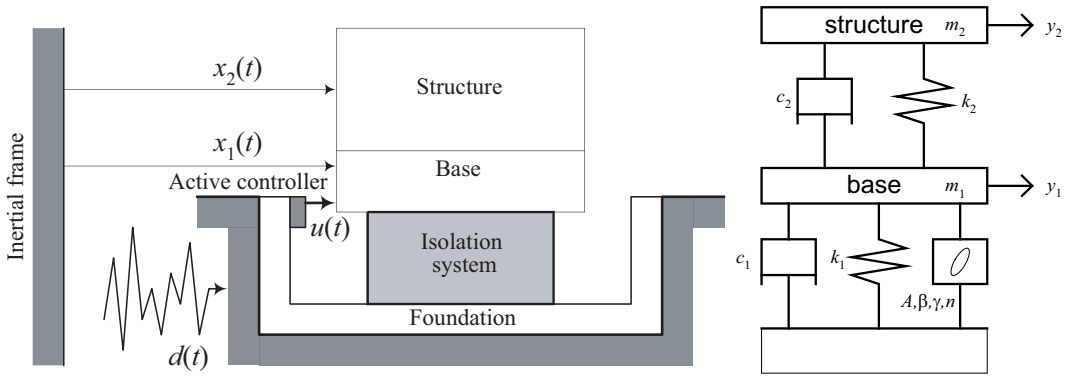

FIGURE 1. Building structure with hybrid control system (left) and physical model (right)

The hysteretic force Φ is described by the Bouc-Wen model [15,16] in the following form:

$$\Phi(x) = \alpha k_0 x + (1-\alpha) D k_0 z \tag{3}$$

$$\dot{z} = D^{-1}\left[A\dot{x} - \beta|\dot{x}||z|^{n-1}z - \phi\dot{x}|z|^n\right] \tag{4}$$

where $\Phi(x,t)$ can be considered as the superposition of an elastic component $\alpha k_0 x(t)$ and a hysteretic component $(1-\alpha)Dk_0 z(t)$, in which $D>0$ is the yield constant displacement and $\alpha \in [0,1]$ is the post to pre-yielding stiffness ratio. The hysteretic part involves a dimensionless auxiliary variable z which is the solution of the nonlinear first order differential Equation (4). In this equation, A, β and ϕ are dimensionless parameters which control the shape and the size of the hysteresis loop, while n is a scalar that governs the smoothness of the transition from elastic to plastic response.

3. **Control Strategy and Controller Design.** Looking at Equation (1), it is clear that a feedback control law can be designed to supply a force u able to control the absolute displacement of the base against the earthquake excitation, which is now a linear combination of the ground displacement and velocity. We may observe that this excitation does not appear in Equation (2), so control of the base motion leads to control of the structure's motion. The origin of the use of absolute coordinates can be found in [1], based on the idea of keeping the whole structure stationary relative to its initial configuration (i.e., relative to an inertial reference frame) and, roughly speaking, "letting the ground move under it".

We consider the following strategy for the feedback control design: measure and regulate the absolute base displacement x_1.

3.1. **Controller design.** In this section, we design a discrete-time backstepping control system for the base isolated uncertain structure in Figure 1. The choice of a discrete-time backstepping adaptive control allows to consider that the parameters of the models are uncertain and to have an upper bound on the asymptotic tracking error – proportional to the sampling period. Furthermore, the control error can be reduced by increasing the design gains up to a certain limit.

In order to use the discrete-time adaptive backstepping approach for the control design, we need to describe the model (1)-(2), along with Equations (3) and (4), in the transfer function form.

3.2. **Model description.** Applying the Laplace transform to Equations (1) and (2) and eliminating the variable x_2, this model, along with Equations (3) and (4), can be written as

$$x_1(t) = \frac{\mathbf{B}(s)}{\mathbf{A}(s)}u(t) + \underbrace{\frac{\mathbf{B}_d^a(s)}{\mathbf{A}(s)}d(t) + \frac{\mathbf{B}_z^a(s)}{\mathbf{A}(s)}z(t)}_{p_a(t)} \tag{5}$$

$$= \frac{\mathbf{B}(s)}{\mathbf{A}(s)}u(t) + p_a(t) \tag{6}$$

where

$$\mathbf{A}(s) = s^4 + \frac{m_1c_2 + c_2m_2 + c_1m_2}{m_1m_2}s^3 + \frac{m_1k_2 + k_1m_2 + k_2m_2 + \alpha k_0 m_2 + c_1c_2}{m_1m_2}s^2$$

$$+\frac{k_1c_2+c_1k_2+\alpha k_0c_2}{m_1m_2}s+\frac{\alpha k_0k_2+k_1k_2}{m_1m_2}$$

$$\mathbf{B}(s)=\frac{1}{m_1}s^2+\frac{c_2}{m_1m_2}s+\frac{k_2}{m_1m_2}$$

$$\mathbf{B}_d^a(s)=\frac{c_1}{m_1}s^3+\frac{k_1m_2+\alpha k_0m_2+c_1c_2}{m_1m_2}s^2$$
$$+\frac{c_2\alpha k_0+k_2c_1+c_2k_1}{m_1m_2}s+\frac{\alpha k_0k_2+k_1k_2}{m_1m_2}$$

$$\mathbf{B}_z^a(s)=\frac{-(1-\alpha)Dk_0}{m_1}s^2+\frac{-c_2(1-\alpha)Dk_0}{m_1m_2}s$$
$$+\frac{-k_2(1-\alpha)Dk_0}{m_1m_2}.$$

In the model (6), we consider both the earthquake motion $d(t)$ and the hysteretic variable $z(t)$ as unknown disturbances. This is why we define the signal $p_a(t)$. The direct transfer function between the control force u and the controlled output is:

$$\frac{\mathbf{B}(s)}{\mathbf{A}(s)}=\frac{b_2s^2+b_1s+b_0}{s^4+a_3s^3+a_2s^2+a_1s+a_0} \tag{7}$$

where the coefficients are

$$b_2=\frac{1}{m_1},$$
$$b_1=\frac{c_2}{m_1m_2},$$
$$b_0=\frac{k_2}{m_1m_2},$$
$$a_3=\frac{m_1c_2+c_2m_2+c_1m_2}{m_1m_2},$$
$$a_2=\frac{k_2m_2+c_1c_2+\alpha k_0m_1+k_1m_2+m_1k_2}{m_1m_2},$$
$$a_1=\frac{k_1c_2+\alpha k_0c_2+c_1k_2}{m_1m_2},$$
$$a_0=\frac{\alpha k_0k_2+k_1k_2}{m_1m_2}.$$

On one hand, we assume that the earthquake motion $d(t)$ is bounded. On the other hand, it has been shown in a previous work [16], that the hysteretic component $z(t)$ is always bounded under a particular choice of the parameters A, β and ϕ ($A>0$, $\beta+\phi>0$, $\beta-\phi\geq 0$ or $A>0$, $\beta-\phi<0$, $\beta\geq 0$).

The boundedness of the signals $d(t)$ and $z(t)$ and the stability of the polynomial expression $\mathbf{A}(s)$ [13] allow us to consider $p_a(t)$ as a *bounded disturbance.*

3.3. **Discrete-time adaptive backstepping control.** Since we consider that the parameters of the models are uncertain, we use adaptive control to stabilize the control loop. Denoting by p anyone of the parameters m_i, k_i, c_i, ($i=1,2$), k_0 and α, we assume that $p\in[p_{\min},p_{\max}]$, $p_{\min}$ and $p_{\max}$ being known, i.e., we assume the knowledge of an interval for each parameter.

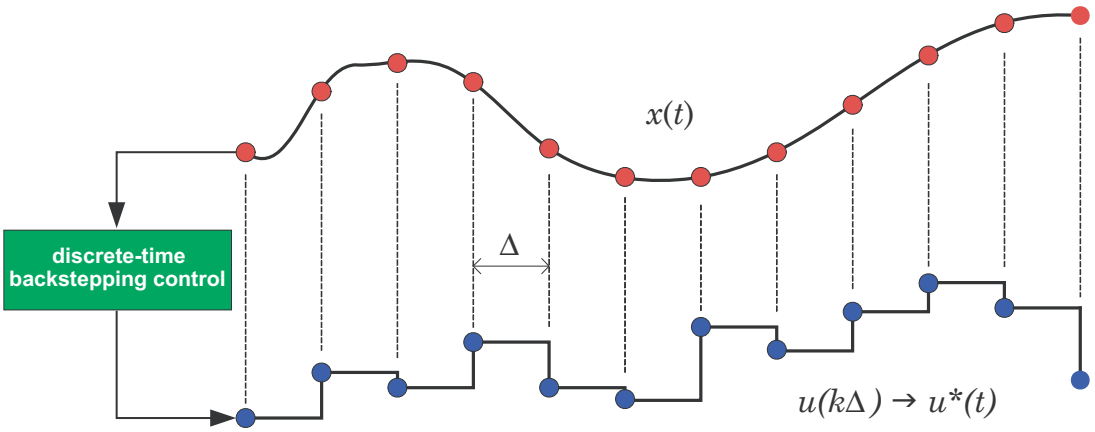

FIGURE 2. The continuous controller $u(t)$ is constructed from the discrete controller $u(k\Delta)$ by using a zero-order hold, that is, $u(t) = u(k\Delta)$, $t \in [k\Delta, (k+1)\Delta)$, $k \geq 0$

In order to digitally implement backstepping adaptive control, we use the discrete-time backstepping approach described in [14]. In this respect, at every sample time $k\Delta$, $k = 0, 1, 2, \ldots$ we measure the absolute base displacement $x_1(k\Delta)$ and compute the corresponding control force $u(k\Delta)$. The continuous controller $u(t)$ is then constructed from the discrete controller $u(k\Delta)$ by using a zero-order hold, as can be seen in Figure 2. Throughout the rest of the paper, the discrete-time signals $w(k\Delta)$ are denoted $w(k)$.

Our objective is to design a continuous control law generated by the zero-order hold such that

(i) all the closed-loop signals remain uniformly bounded,
(ii) the plant output $x_1(t)$ tracks as closely as possible the reference signal $x_r(t)$.

Figure 3 summarizes the step-by-step algorithm that, starting from the discrete-time measurement $x_1(k\Delta)$, ends up with the computation of the discrete-time control value $u(k\Delta)$. The details of the derivations and some of the variables of this algorithm are omitted for space reasons, but the complete developments and definitions can be found in [14]. For the practical use of the control algorithm, it is important to remark that the quantities ζ_1, ζ_2, ι_1, ι_2, $\sigma_{s\theta}$, $\sigma_{s\varrho}$ and γ are positive design parameters, Γ is a 7-dimensional square matrix, and M_θ, M_ϱ are defined as

$$M_\theta = \sqrt{\sum_{i=0}^{3} a_i^2 + \sum_{i=0}^{2} b_i^2}, \quad M_\varrho = |1/b_2|.$$

3.4. **Robustness analysis.** In this section we summarize the robustness and asymptotic performance results which are derived following the reference by [14, Theorem 6.1].

If we consider the system (6) and the discrete-time adaptive controller composed of the control law and the parameter update law described in Figure 3, then there exists a real $\Delta^* > 0$, a positive integer q, and a positive constant c independent of Δ and the initial conditions such that, for:

(i) $0 \leq \Delta \leq \Delta^*$;
(ii) $\|\lambda(0), \chi(0)\| \leq c/\Delta^{1/2q}$,
(iii) $\|x_r\|_\infty + \|\delta x_r\|_\infty + \|\delta^2 x_r\|_\infty \leq c/\Delta^{1/2q}$,

the following holds:

(1) all the signals (discrete and continuous) of the closed loop remain bounded,

Error variables

$$z_1(k) = y(k) - y_r(k), \quad z_2(k) = v_{2,2}(k) - \hat{\varrho}(k)\delta y_r(k) - \alpha_1(k)$$

Stabilizing functions

$$\alpha_1(k) = \hat{\varrho}(k)\bar{\alpha}_1(k)$$

$$\bar{\alpha}_1(k) = -(\zeta_1 + \iota_1)z_1(k) - \xi_{4,2}(k) - \bar{\omega}^{\mathrm{T}}(k)\hat{\theta}(k)$$

$$\alpha_2(k) = -\hat{b}_2 z_1(k) - \left[\zeta_2 + \iota_2\left(\frac{\partial\alpha_1}{\partial y}\right)^2\right] z_2(k) + \beta_2(k) + \frac{\partial\alpha_1}{\partial\hat{\theta}}\tau_2(k)$$

$$\beta_2(k) = \frac{\partial\alpha_1}{\partial y}(\xi_{4,2}(k) + \omega^{\mathrm{T}}(k)\hat{\theta}(k)) + \frac{\partial\alpha_1}{\partial\eta}(A_0\eta(k) + e_4 y(k)) + \frac{\partial\alpha_1}{\partial y_r}\delta y_r(k) + \kappa_2 v_{2,1}(k) + \frac{\partial\alpha_1}{\partial\lambda_1}(-\kappa_1\lambda_1(k) + \lambda_2(k)) + \frac{\partial\alpha_1}{\partial\lambda_2}(-\kappa_2\lambda_1(k) + \lambda_3(k)) + \frac{\partial\alpha_1}{\partial\lambda_3}(-\kappa_3\lambda_1(k) + \lambda_4(k)) - \left(\delta y_r(k) + \frac{\partial\alpha_1}{\partial\hat{\varrho}}\right)\delta\hat{\varrho}(k)$$

Tuning functions

$$\tau_1(k) = \Gamma(\omega(k) - \hat{\varrho}(k)(\delta y_r(k) + \bar{\alpha}_1(k))e_1)z_1(k) - \Gamma\sigma_\theta(\|\hat{\theta}\|)\hat{\theta}(k),$$

$$\tau_2(k) = \tau_1(k) - \Gamma\frac{\partial\alpha_1}{\partial y}\omega(k)z_2(k)$$

Parameter update laws

$$\delta\hat{\theta}(k) = \tau_2(k),$$

$$\delta\hat{\varrho}(k) = -\gamma\,\mathrm{sgn}(b_2)\,(\delta y_r(k) + \bar{\alpha}_1(k))\,z_1(k) - \gamma\sigma_\varrho(|\hat{\varrho}|)\,\hat{\varrho}(k)$$

Switching σ-modification

$$\sigma_\theta(\|\hat{\theta}\|) = \begin{cases} 0, & \|\hat{\theta}\| \le M_\theta \\ \sigma_{s\theta}, & \|\hat{\theta}\| \ge 2M_\theta \\ \text{smooth connecting function,} & \text{otherwise} \end{cases}$$

$$\sigma_\varrho(|\hat{\varrho}|) = \begin{cases} 0, & |\hat{\varrho}| \le M_\varrho \\ \sigma_{s\varrho}, & |\hat{\varrho}| \ge 2M_\varrho \\ \text{smooth connecting function,} & \text{otherwise} \end{cases}$$

Adaptive control law

$$u(k) = \alpha_2(k) - v_{2,3}(k) + \hat{\varrho}(k)\delta^2 y_r(k)$$

FIGURE 3. Discrete tuning functions control algorithm

(2) the magnitude of the output is proportional to the sampling rate according to:

$$\limsup_{t\to\infty} x_1^2(t) \le c\frac{\sqrt{\Delta} + \sigma_{s\theta} + \sigma_{s\varrho}}{\alpha}, \tag{8}$$

where α is a known function of, among others, the design parameters ζ_1, ζ_2, ι_1, ι_2, and $\chi(0)$ is a vector of initial conditions.

On one hand, the condition in **(i)** states that the choice of the sampling time is limited by an unknown positive real number Δ^*. On the other hand, conditions **(ii)** and **(iii)** establish a limitation in the region of initial conditions and in the amplitude of the reference

signal and its derivatives. However, in the numerical simulations, these last two conditions are trivially satisfied because we have chosen zero-initial conditions and a constant zero function as a reference signal. From a practical point of view, the implementation of the discrete-time backstepping control requires the choice of the sampling time Δ, the positive constants ζ_1, ζ_2, ι_1, ι_2, $\sigma_{s\theta}$, $\sigma_{s\varrho}$ and γ.

4. **Numerical Simulations.** In this section the control algorithm is applied to the design model presented in Section 2 and to an eight-storied building structure.

4.1. **Base-isolated single degree of freedom model.** Consider the system in Figure 1, whose parameters are listed in Table 1. The hysteretic parameters are also described in Table 2. We remark that this particular choice of the hysteretic parameters satisfies $A > 0$, $\beta + \phi > 0$ and $\beta - \phi \geq 0$, that is, the hysteretic component $z(t)$ will be always bounded, as can be seen in [16]. In order to investigate the efficiency of the proposed control algorithm on this simple structure, we consider the 1952 Taft earthquake.

Figure 4 displays the time histories of the motions of the base (displacement and acceleration) and the control signal force for the control design using a sampling period

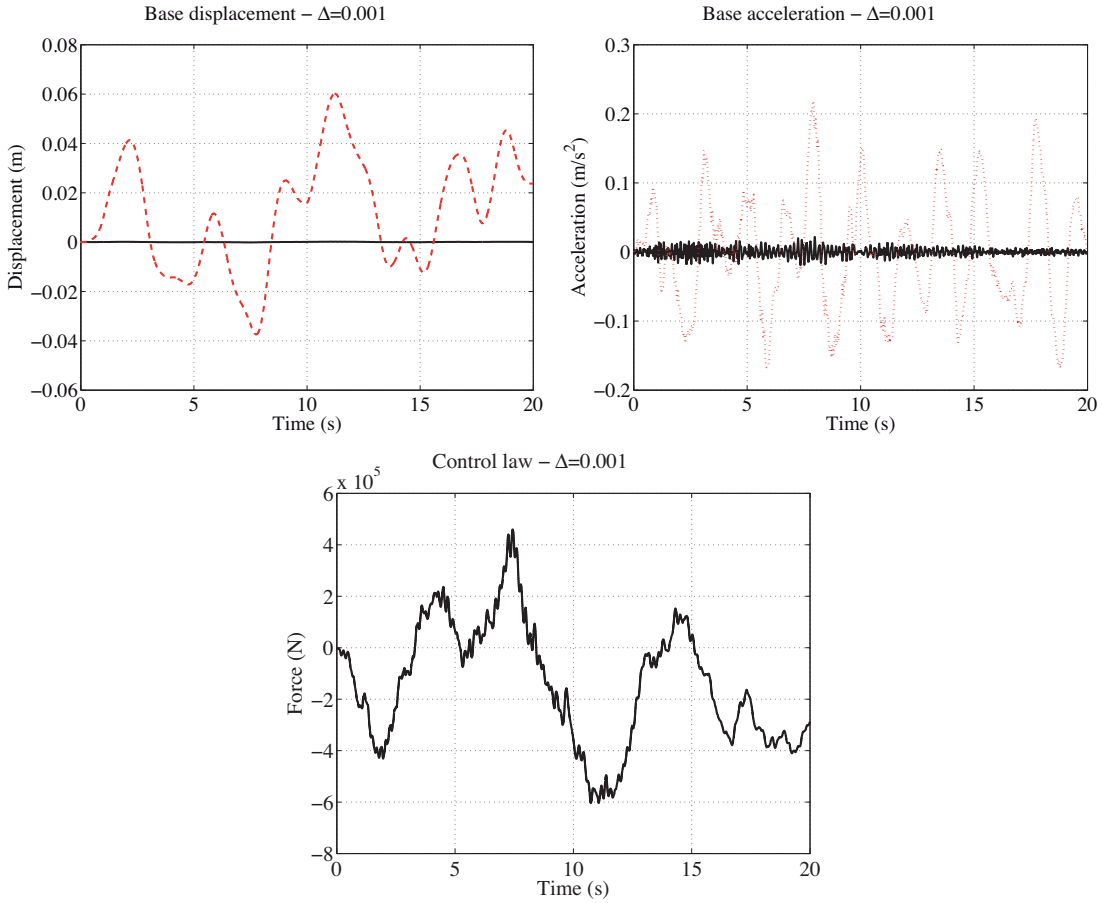

FIGURE 4. Numerical simulations with sampling time $\Delta = 0.001$ s and design parameters $\zeta_i = \iota_i = 6$, $i = 1, 2$. Closed loop base displacement (solid) and open loop base displacement (dashed) (m) (top, left); closed loop base acceleration (solid) and open loop base acceleration (dashed) (m/s^2) (top, right); control signal force, $u(t)$ (N) (down).

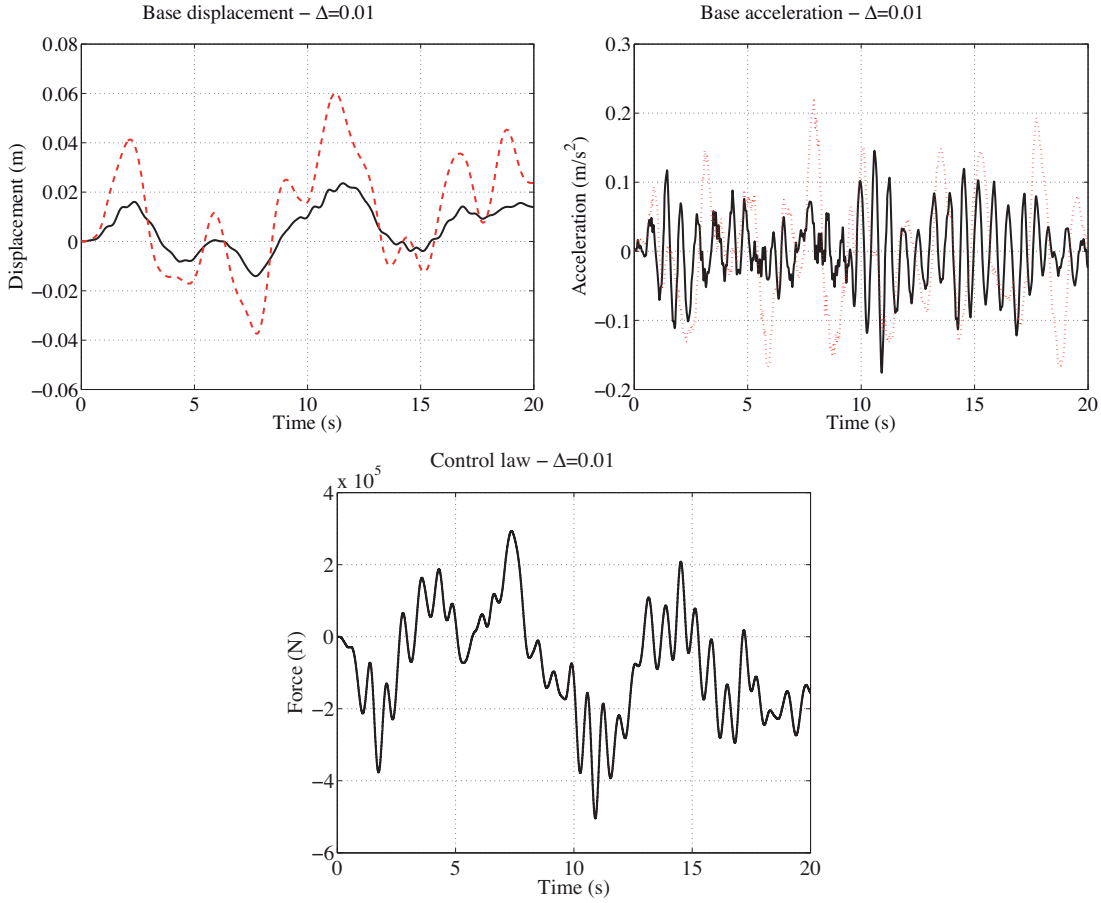

FIGURE 5. Numerical simulations with sampling time $\Delta = 0.01$ s and design parameters $\zeta_i = \iota_i = 1.3$, $i = 1, 2$. Closed loop base displacement (solid) and open loop base displacement (dashed) (m) (top, left); closed loop base acceleration (solid) and open loop base acceleration (dashed) (m/s^2) (top, right); control signal force, $u(t)$ (N) (down).

TABLE 1. Model coefficients of the single-degree-of-freedom system

	base	**structure**
mass	$m_1 = 6 \times 10^5$ kg	$m_2 = 6 \times 10^5$ kg
stiffness	$k_1 = 0.1185 \times 10^8$ N/m	$k_2 = 9 \times 10^8$ N/m
damping	$c_1 = 0.1067 \times 10^7$ Ns/m	$c_2 = 0.2324 \times 10^7$ Ns/m

TABLE 2. Parameters of the hysteresis model

$\alpha = 0.5$	$A = 1$
$k_0 = 61224.49$ N/m	$\beta = 0.5$
$D = 0.0245$ m	$\phi = 0.5$

$\Delta = 0.001$ s and design parameters $\zeta_i = \iota_i = 6$, $i = 1, 2$. Figure 5 gives the same information for the control system using a sampling time $\Delta = 0.01$ s and design parameters $\zeta_i = \iota_i = 1.3$, $i = 1, 2$.

Looking at Figure 4, it can be seen that the controlled absolute displacement and acceleration are drastically reduced compared with the uncontrolled case. The control action lies within the range of acceptable values.

In the numerical experiments in Figure 5 the sampling time is $\Delta = 0.01$ s (ten times greater). It is observed that the reduction is not as drastic as for $\Delta = 0.001$ s but it is still significant, while the acceleration reduction is small. The control action is smaller and smoother than for the previous case. The bigger reduction in the displacement for the smaller sampling period is understandable according to the inequality (8). This inequality also indicates that the displacement reduction can rely on increasing the value of α. Although the details are omitted in the paper for space reasons, it can be shown that the value of α can be increased by increasing the values of the design parameters ζ_1, ι_1, ζ_2, ι_2. However, this increase and the corresponding base displacement reduction cannot be arbitrarily big. A practical limit exists beyond which the closed loop becomes unstable. In Figure 6, for a fixed $\Delta = 0.01$ s, the control parameters are moved from 0.7 to 1.3. We observe that the bigger control parameters, the bigger reduction displacement. Beyond 1.3, the closed loop becomes unstable.

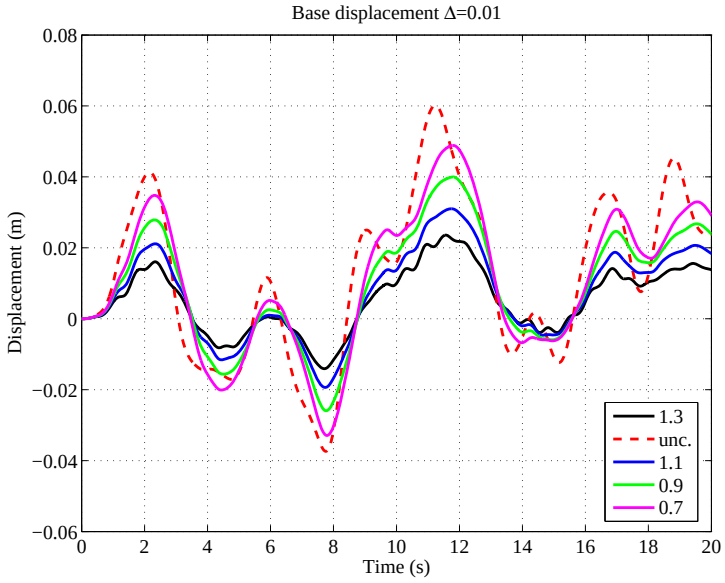

FIGURE 6. For a fixed sampling period Δ, the magnitude of the output can be reduced by increasing the design gains up to a certain limit (0.7, 0.9, 1.1 and 1.3)

TABLE 3. Model coefficients of the base-isolated structure

	mass (t)	**stiffness** (N/m)	**damping** (Ns/m)
base	3565.7	919422	101439
1st floor	2580	12913000	11363
2nd floor	2247	10431000	10213
3rd floor	2057	7928600	8904
4th floor	2051	5743900	7578
5th floor	2051	3292800	5738
6th floor	2051	1674400	4092
7th floor	2051	496420	2228
8th floor	2051	49620	704

The designer needs to appropriately fix the sampling time and the control parameters within the technical restrictions and the expected performance.

4.2. **Eighth-storied building structure.** As a more realistic example, we consider now a hysteretic base-isolated eight-storied building, whose parameters are listed in Table 3. This building structure is illustrated in Figure 7. For control design, a dynamic model composed of two coupled subsystems, namely the main structure or superstructure (S_r) and the base isolation (S_c) is employed:

$$\begin{aligned} S_r :& \mathbf{M}\ddot{\mathbf{x}}_\mathbf{r} + \mathbf{C}\dot{\mathbf{x}}_\mathbf{r} + \mathbf{K}\mathbf{x}_\mathbf{r} = 0, \\ S_c :& m_0\ddot{x}_0 + (\bar{c}_0 + c_1)\dot{x}_0 + (\bar{k}_0 + k_1)x_0 = \\ & k_1 x_1 + c_1\dot{x}_1 - \Phi(x_0 - x_g, t) + \bar{c}_0\dot{x}_g + \bar{k}_0 x_g + u, \end{aligned}$$

where x_g and $\dot{x}_g$ are the displacement and velocity of the seismic ground motion, respectively, $\mathbf{x_r} = [x_1, x_2, \ldots, x_8]^{\mathrm{T}} \in \mathbb{R}^8$ represents the horizontal absolute displacement with respect to an inertial frame. The mass, damping and stiffness of the ith story is denoted by m_i, c_i and k_i, respectively. The base isolation is described as a single degree of freedom with horizontal absolute displacement x_0. It is assumed to exhibit a linear behavior characterized by mass, damping, stiffness m_0, $\bar{c}_0$ and $\bar{k}_0$, respectively, plus a nonlinear behavior represented by a hysteretic restoring force $\Phi(x_0 - x_g, t)$. The matrices $\mathbf{M}$, $\mathbf{C}$ and $\mathbf{K}$ of the structure have the following form

$$\mathbf{M} = \operatorname{diag}(m_1, m_2, \ldots, m_8) \in \mathbb{R}^{8\times 8},$$

$$\mathbf{C} = \begin{bmatrix} c_1 + c_2 & -c_2 & 0 & \cdots & 0 & 0 \\ -c_2 & c_2 + c_3 & -c_3 & \cdots & 0 & 0 \\ \vdots & \vdots & \vdots & \cdots & \vdots & \vdots \\ 0 & 0 & 0 & \cdots & -c_8 & c_8 \end{bmatrix} \in \mathbb{R}^{8\times 8},$$

$$\mathbf{K} = \begin{bmatrix} k_1 + k_2 & -k_2 & 0 & \cdots & 0 & 0 \\ -k_2 & k_2 + k_3 & -k_3 & \cdots & 0 & 0 \\ \vdots & \vdots & \vdots & \cdots & \vdots & \vdots \\ 0 & 0 & 0 & \cdots & -k_8 & k_8 \end{bmatrix} \in \mathbb{R}^{8\times 8}.$$

The restoring force Φ can be represented by the Bouc-Wen model as in Equations (3) and (4), whose parameters are described in Table 2.

Finally, u is the control force supplied by an appropriate actuator.

The following equations of motion of the base and the first floor will be used in the controller design:

$$\begin{aligned} S_{r_1} :& m_1\ddot{x}_1 + (c_1 + c_2)\dot{x}_1 + (k_1 + k_2)x_1 = \\ & c_1\dot{x}_0 + k_1 x_0 + c_2\dot{x}_2 + k_2 x_2, \\ S_c :& m_0\ddot{x}_0 + (\bar{c}_0 + c_1)\dot{x}_0 + (\bar{k}_0 + k_1)x_0 = \\ & k_1 x_1 + c_1\dot{x}_1 - \Phi(x_0 - x_g, t) + \bar{c}_0\dot{x}_g + \bar{k}_0 x_g + u, \end{aligned}$$

or, equivalently,

$$\begin{aligned} S_{r_1} :& m_1\ddot{x}_1 + c_1\dot{x}_1 + k_1 x_1 = \\ & c_1\dot{x}_0 + k_1 x_0 + \underbrace{c_2(\dot{x}_2 - \dot{x}_1) + k_2(x_2 - x_1)}_{\varepsilon[x_1, \dot{x}_1, x_2, \dot{x}_2]}, \end{aligned} \tag{9}$$

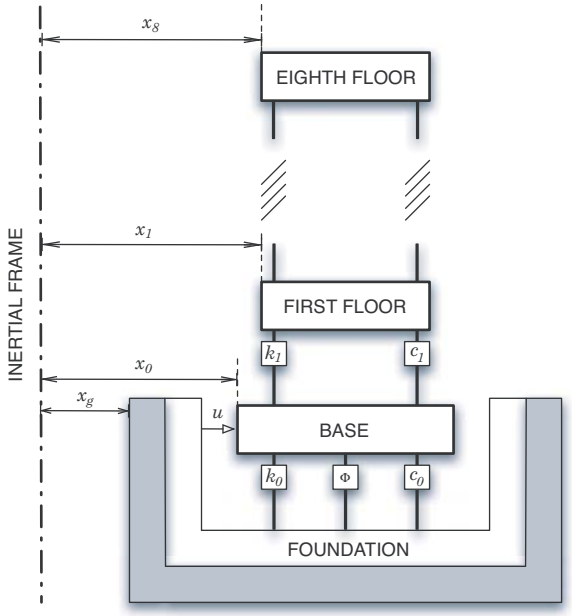

FIGURE 7. Base-isolated structure with active control

$$S_c : m_0\ddot{x}_0 + (\bar{c}_0 + c_1)\dot{x}_0 + (\bar{k}_0 + k_1)x_0 = k_1x_1 + c_1\dot{x}_1 - \Phi(x_0 - x_g, t) + \bar{c}_0\dot{x}_g + \bar{k}_0x_g + u. \tag{10}$$

It is well accepted that the movement of the superstructure S_r is very close to the one of a rigid body due to the base isolation [17]. Then it is reasonable to assume that the inter-story motion of the building, and in particular $\dot{x}_2 - \dot{x}_1$ and $x_2 - x_1$ will be much smaller than the absolute motion of the base [10]. Hence, the right-hand terms of S_{r_1} in Equation (9) can be simplified as

$$c_1\dot{x}_0 + k_1x_0 + \varepsilon[x_1, \dot{x}_1, x_2, \dot{x}_2] \approx c_1\dot{x}_0 + k_1x_0.$$

Consequently, the following simplified equation of motion of the first floor, together with the equation of motion of the base, can be used in the subsequent controller design:

$$S_{r_1} : m_1\ddot{x}_1 + c_1\dot{x}_1 + k_1x_1 = c_1\dot{x}_0 + k_1x_0, \tag{11}$$

$$S_c : m_0\ddot{x}_0 + (\bar{c}_0 + c_1)\dot{x}_0 + (\bar{k}_0 + k_1)x_0 = k_1x_1 + c_1\dot{x}_1 - \Phi(x_0 - x_g, t) + \bar{c}_0\dot{x}_g + \bar{k}_0x_g + u. \tag{12}$$

Now, applying the Laplace transform to Equations (11) and (12) and eliminating the variable x_1, this model can be written as

$$x_0(s) = \frac{\mathbf{B}(s)}{\mathbf{A}(s)}u(s) + p_a(t)$$

and consequently the same discrete time adaptive control described in Section 3.3 can be applied to this structure.

In this case, in order to investigate the efficiency of the proposed control scheme, the controlled structure is simulated for two earthquake ground accelerations: Newhall (1994) and Kobe (1995).

Figures 8 and 9 display the time histories of the motions of the base (displacement and acceleration) and the control signal force for the control design using a sampling period of $\Delta = 0.01$ s and design parameters $\zeta_i = \iota_i = 1.5$, $i = 1, 2$, for both Newhall and Kobe earthquakes. The benefit of this active control strategy is the significant reduction of

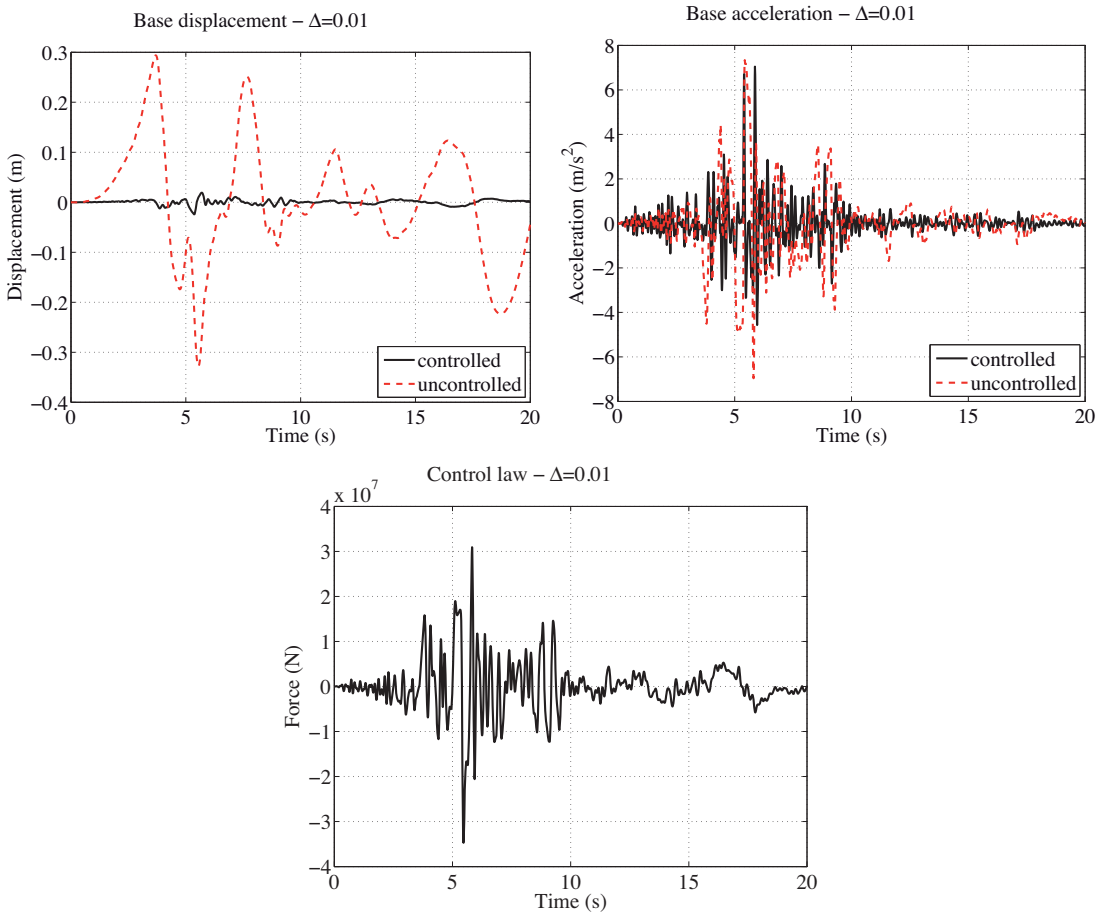

FIGURE 8. Numerical simulations of the eight-storey building in Section 4.2 under Newhall excitation with sampling time $\Delta = 0.01$ s and design parameters $\zeta_i = \iota_i = 1.5$, $i = 1, 2$. Closed loop base displacement (solid) and open loop base displacement (dashed) (m) (top, left); closed loop base acceleration (solid) and open loop base acceleration (dashed) (m/s^2) (top, right); control signal force, $u(t)$ (N) (down).

the base displacement without increase in accelerations. Hence, a controller that reduces or does not increase accelerations while reducing the base displacement significantly, is desirable for practical applications.

5. **Conclusions.** The paper has presented an active control scheme for hysteretic base isolated structures. An adaptive backstepping control is formulated in continuous time based on a model of the system in absolute coordinates. The control law is discretized into a digital control algorithm. The implementation of this algorithm along with a zero-order hold is able to keep uniformly all the signals of the closed loop within certain bounds and to give an upper bound of the asymptotic tracking error. These bounds are related to the sampling period.

Acknowledgment. This work is supported by CICYT (Spanish Ministry of Science and Innovation) through grant number DPI2011-28033-C03-01.

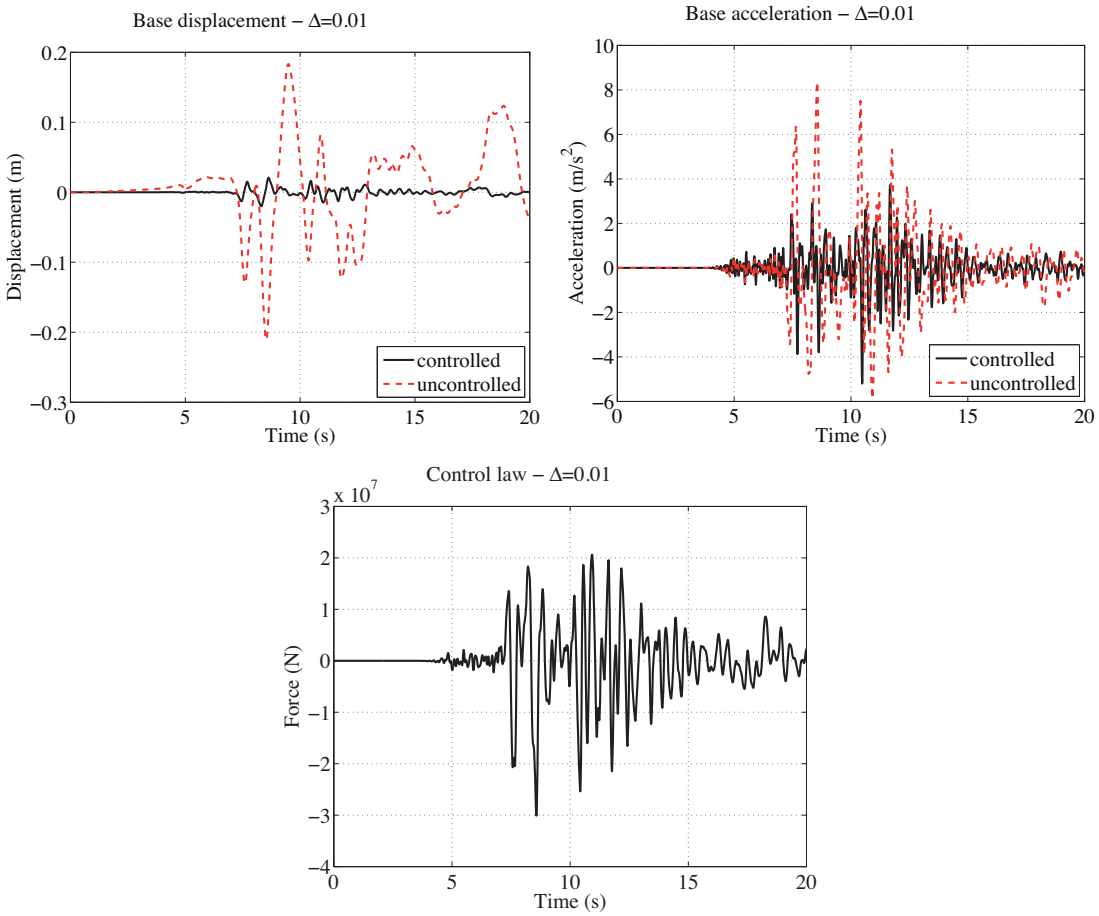

FIGURE 9. Numerical simulations of the eight-story building in Section 4.2 under Kobe excitation with sampling time $\Delta = 0.01$ s and design parameters $\zeta_i = \iota_i = 1.5$, $i = 1, 2$. Closed loop base displacement (solid) and open loop base displacement (dashed) (m) (top, left); closed loop base acceleration (solid) and open loop base acceleration (dashed) (m/s^2) (top, right); control signal force, $u(t)$ (N) (down).

REFERENCES

[1] J. Kelly, G. Leitmann and A. Soldatos, Robust control of base-isolated structures under earthquake excitation, *Journal of Optimization Theory and Applications*, vol.53, no.2, pp.159-180, 1987.

[2] J. Inaudi, F. Lopez-Almansa, J. Kelly and J. Rodellar, Predictive control of base-isolated structures, *Earthquake Engineering and Structural Dynamics*, vol.21, pp.471-482, 1992.

[3] L. Jansen and S. Dyke, Semiactive control strategies for MR dampers: Comparative study, *Journal of Engineering Mechanics*, vol.126, no.8, pp.795-803, 2000.

[4] J. Ramallo, E. Johnson and B. Spencer, Smart base isolation systems, *Journal of Engineering Mechanics*, vol.128, pp.1088-1099, 2002.

[5] S. Narasimhan, S. Nagarajaiah, E. Johnson and H. Gavin, Smart base isolated benchmark building. Part I: Problem definition, *Journal of Structural Control and Health Monitoring*, vol.13, no.2-3, pp.573-588, 2006.

[6] L. Acho and F. Pozo, Sliding mode control of hysteretic structural systems, *International Journal of Innovative Computing, Information and Control*, vol.5, no.4, pp.1081-1087, 2009.

[7] F. Pozo, P. M. Montserrat, J. Rodellar and L. Acho, Robust active control of hysteretic base-isolated structures: Application to the benchmark smart base-isolated building, *Structural Control and Health Monitoring*, vol.15, no.5, pp.720-736, 2008.

[8] H. Irschik, K. Schlacher and A. Kugi, Control of earthquake excited nonlinear structures using Lyapunov's theory, *Computers and Structures*, vol.67, pp.83-90, 1998.
[9] N. Luo, J. Rodellar, M. D. la Sen and J. Vehí, Output feedback sliding mode control of base isolated structures, *Journal of the Franklin Institute*, vol.337, pp.555-577, 2000.
[10] N. Luo, J. Rodellar, J. Vehí and M. D. la Sen, Composite semiactive control of a class of seismically excited structures, *Journal of the Franklin Institute*, vol.338, pp.225-240, 2001.
[11] M. Krstić, I. Kanellakopoulos and P. Kokotović, *Nonlinear and Adaptive Control Design*, John Wiley & Sons, 1995.
[12] S. Tong, N. Sheng and Y. Li, Observer-based adaptive fuzzy backstepping control for strict-feedback nonlinear systems with unknown time delays, *International Journal of Innovative Computing, Information and Control*, vol.7, no.12, pp.6949-6964, 2011.
[13] F. Pozo, F. Ikhouane, J. Rodellar and G. Pujol, Adaptive backstepping control of hysteretic base-isolated structures, *Journal of Vibration and Control*, vol.12, no.4, pp.373-394, 2006.
[14] A. Rabeh, F. Ikhouane and F. Giri, An approach to digital implementation of continuous backstepping adaptive control for linear systems, *International Journal of Adaptive Control and Signal Processing*, vol.13, no.5, pp.327-346, 1999.
[15] F. Ikhouane and J. Rodellar, On the hysteretic Bouc-Wen model. Part I: Forced limit cycle characterization, *Nonlinear Dynamics*, vol.42, no.1, pp.63-78, 2005.
[16] F. Ikhouane and J. Rodellar, *Systems with Hysteresis: Analysis, Identification and Control Using the Bouc-Wen Model*, John Wiley & Sons, Chichester, UK, 2007.
[17] R. I. Skinner, G. H. Robinson and G. H. McVerry, *An Introduction to Seismic Isolation*, John Wiley & Sons, Chichester, UK, 1992.